



Microbiotas from UC patients display altered metabolism and reduced ability of LAB to colonize mucus

Louise Kristine Vignsnaes^{1*}, Pieter van den Abbeele^{2*}, Karolina Sulek¹, Henrik Lauritz Frandsen¹, Casper Steenholdt³, Jørn Brynskov³, Joan Vermeiren², Tom van de Wiele² & Tine Rask Licht¹

¹National Food Institute, Technical University of Denmark, Mørkhøj Bygade 26, DK-2860 Søborg, Denmark, ²Laboratory of Microbial Ecology and Technology (LabMET), Ghent University, Coupure Links 653, B-9000 Gent, Belgium, ³Department of Gastroenterology, Herlev Hospital, DK-2730 Herlev, Denmark.

We compared fecal microbial communities derived either from Ulcerative Colitis (UC) patients in remission (n=4) or in relapse (n=4), or from healthy subjects (n=4). These communities were used for inoculation of a dynamic *in vitro* gut model, which contained integrated mucin-covered microcosms. We found that the microbiota of the 'mucus' largely differed from that of the 'lumen'. This was partly due to decreased mucus-associated populations of lactic acid producing bacterial populations (LAB), as LAB originating from UC patients had a significantly decreased capacity to colonize the mucin-covered microcosms as compared to those originating from healthy subjects. We found significant differences between the metabolomes of UC patients in relapse and remission, respectively, while the metabolome of patients in remission resembled that of healthy subjects. These novel findings constitute an important contribution to the understanding of the complex etiology of UC.

The mucus layer lining the epithelium of the gastrointestinal tract is important for the protection of the intestinal epithelium in humans. Commensal bacteria have been found to colonize the colonic mucus layer, and previous studies have shown that the microbial community found in the colonic mucus differs from that of the luminal community^{1,2}. Several microbial characteristics have contributed to the evolution of the specifically selected mucosal community, including the ability of the bacteria to utilize mucin glycans as energy source as well as resistance to nonspecific antimicrobial peptides and specific antimicrobial immunoglobulins produced by the host^{3,4}. Additionally, many adhesion molecules expressed by colonic bacteria have mucin glycans as specific epitopes^{5,6}, and it has been suggested that the glycosylation pattern in mucin, hence the attachment site and energy source for the colonic bacteria, is an important factor for host selection of a specific mucosal community³. Lack or defects in the mucosal barrier may allow bacteria to reach the epithelium and trigger colonic inflammation.

Ulcerative colitis (UC) is an idiopathic inflammatory bowel disease characterized by chronic relapsing inflammation of the colonic mucosa⁷. The etiology of UC remains an enigma, and no known infectious agent has been demonstrated^{8,9}. It has been speculated that UC originates from a dysregulated immune response to the commensal intestinal microbiota in genetically susceptible individuals^{10,11}. Human studies have revealed that UC patients have a colonic mucus layer that has an altered O-glycan profile and is significantly thinner than that of healthy subjects, which may select for a different mucosal microbial profile^{12,13}. Consistently, several studies have shown that patients with UC have an altered bacterial microbiota^{14–18}. Thus, the bacterial and/or host-bacterial interactions may play a role in the pathogenesis of UC.

In vitro models are well-suited to screen the adhering potency of intestinal microbes. They include adhesion assays to various components of the intestinal surface: e.g. intestinal mucus¹⁹, mucins²⁰, colonic tissue²¹ or cell lines²². A drawback to such models is that they often provide only short-term information based on axenic cultures and thus ignore the interactions between and within the luminal and mucosal microbial communities. Therefore, a dynamic *in vitro* gut model has been developed, which simulates both the luminal and mucosal environment²³. This model, named the M-SHIME was adapted from the validated Simulator of the Human Intestinal Microbial Ecosystem (SHIME)²⁴. Compared to earlier *in vitro* models, the M-SHIME allows a more representative colonization of specific *Lactobacillus* sp²³. Furthermore, high-resolution phylogenetic microbiota profiling shows that the simulated mucosal microbiota is, in correspondence with *in vivo* studies, enriched with

SUBJECT AREAS:
BACTERIAL ADHESION
MICROBIAL ECOLOGY
CLINICAL MICROBIOLOGY
MOLECULAR BIOLOGY

Received
9 November 2012

Accepted
6 December 2012

Published
23 January 2013

Correspondence and requests for materials should be addressed to T.R.L. (trli@food.dtu.dk)

* These authors contributed equally to this work.



Firmicutes belonging to the Clostridial clusters IV and XIVa²⁴. Moreover, the *in vitro* mucosal environment is necessary to avoid the wash-out of specific surface-associated microbes, which occurs in conventional *in vitro* models. Hence, the M-SHIME allows studies of the mucosal microbiota and the interaction between luminal and mucosal microbial communities.

The aims of this study were (1) to investigate the ability of fecal microbiota from healthy subjects and UC patients in either remission or relapse to colonize the artificial mucus layer of the M-SHIME and (2) to elucidate microbial activity by comparison of metabolic profiles of the luminal and mucosal microbial communities derived from UC patients and healthy subjects. Denaturing Gradient Gel Electrophoresis (DGGE) and quantitative Real-Time PCR (qPCR), both of which are culture-independent methods, were applied for microbiota analysis, while Liquid Chromatography – Mass Spectroscopy (LC-MS) was used to analyze the potential role of extracellular metabolites produced by microorganisms in the lumen and mucus of the M-SHIME.

Results

Microbial activity in terms of SCFA production. SCFA were analyzed in the luminal content of the colonic M-SHIME vessels as a measure of the metabolic activity of the microbiota derived from healthy subjects or UC patients, either in remission or relapse (Table 1). Forty-two hours after inoculation with fecal samples, there was a significant inter-individual variability within each group regarding the conversion of the provided nutrients to SCFA ($P < 0.05$). As a result of this variability, no significant differences were detectable between the three groups. However, there was a trend of lower acetate and higher branched SCFA concentrations for UC patients as opposed to healthy subjects ($P = 0.138$ and $P = 0.210$, respectively). Additionally, we found it noteworthy that the levels of carboxyproate found in samples containing microbiota from patients in remission was 36 fold higher than in samples with microbiota from patients in relapse ($P = 0.229$).

Microbial community analysis using DGGE. Comparison of DGGE profiles containing 16S ribosomal genes amplified from luminal and mucosal samples of healthy subjects and UC patients after 42 h colonization revealed a distinct difference between the dominant bacterial members of the luminal and mucosal environment (Figure 1). The dendrogram from the Dice cluster analysis showed three clusters with all mucosal samples in cluster I (54.61% similarity), five luminal samples in cluster II (53.89% similarity), and seven luminal samples in cluster III (41.15% similarity). Clustering of the distribution of these dominant microbial species did not correlate to the health status of the human subjects (healthy, UC in remission and UC in relapse).

Microbial community analysis by qPCR. For microbiotas derived from UC patients in relapse or remission, luminal and mucosal samples were separated from one another, while this separation

was not equally clear for samples from healthy subjects (Figure 2, score plot). *Roseburia*, *Faecalibacterium prausnitzii*, and *Clostridiaceae/Eubacterium* represented samples from the mucosal environment, while *B. bifidum*, *B. adolescentis*, *Bifidobacterium* spp., *Lactobacillus* spp., *Akk. muciniphila* and *Actinobacteria* represented the luminal content samples (Figure 2, loading plot).

It was noteworthy that the preference of specific bacterial groups to colonize the mucosal and/or luminal compartment was clearly affected by the origin of the microbiota (healthy subjects, UC patients in remission or UC patients in relapse) (Table 2). No significant differences between the luminal and mucosal samples with respect to proportions of specific bacterial taxa were measured when fecal communities were derived from healthy subjects. However, in the vessels with communities derived from UC patients in relapse, mucus was colonized by significantly lower proportions of bifidobacteria, *B. bifidum*, lactobacilli, *C. coccoides* group, *C. leptum* subgroup and *Alistipes* spp. ($P = 0.01$, $P = 0.02$, $P = 0.03$, $P = 0.05$, $P = 0.02$, and $P = 0.05$, respectively) than found in lumen. Additionally, the densities of bifidobacteria, *B. adolescentis*, *B. pseudocatenulatum*, lactobacilli, *C. leptum* subgroup, *Faecalibacterium prausnitzii* and *Actinobacteria* derived from UC patients in remission were significantly lower in mucus than in lumen ($P = 0.01$, $P = 0.001$, $P = 0.01$, $P = 0.007$ and $P = 0.05$, $P = 0.03$ and $P = 0.001$, respectively). Finally, significantly higher mucosal counts of *Roseburia* spp. derived from UC patients in remission were measured ($P = 0.05$).

Comparison of the proportions of specific taxa present in the luminal and mucosal compartments, respectively, from the three types of microbiota (healthy, UC remission, UC relapse) revealed that relative quantities of *Bifidobacterium* spp. and *Lactobacillus* spp. in mucus was significantly lower ($P = 0.05$ and $P = 0.002$, respectively) in communities derived from UC patients in relapse than in those derived from healthy subjects, whereas the relative quantity of *Clostridiaceae/Eubacterium* was significantly higher in the lumen ($P = 0.04$) in communities from UC patients in relapse than in those from healthy subjects (Table 3).

The bacterial growth rate of selected bacterial taxa in the lumen was calculated from the slope of the exponential phase of the growth curves. The growth rate was increased during the 42 h incubation in the lumen for all the examined bacterial taxa. No significant difference in the growth rate for each bacterial taxon was found when comparing the three groups (healthy subjects, UC in remission or UC in relapse) (Table S3, supplementary data).

Metabolite detection and separation. PCA of the metabolites as detected by LCMS revealed a difference between samples taken from healthy subjects and UC patients in relapse, respectively. The grouping was present in samples from mucus (Figure 3, score plot) as well as from lumen (Figure 4, score plot). No difference was observed between UC patients in remission and healthy subjects (Figure S1 and S2, supplementary data). However, a clear separation between score plots for UC patients in relapse and remission, respectively, was seen (Figure S3 and S4, supplementary data).

Based on the PCA loading plots (Figure 3 and 4), metabolites, which were tentatively causative for the difference observed between UC patients in relapse and healthy subjects, were identified (Table 4 and 5). Loadings, which in extracted ion chromatograms showed clear chromatogram peaks (data not shown) that were present in significantly different levels ($P < 0.05$) in the two groups were further investigated. Substances in the Human Metabolome Database, which corresponded to the found mass/charge ratio (M_{LCMS}) were identified. However, a few of the given mass/charge values had more than one possible match (Table 4 and 5).

Discussion

In this study, we applied a recently developed dynamic *in vitro* gut model, the M-SHIME, to investigate differences between the

Table 1 | The average (\pm SEM) absolute SCFA levels (mM) in the luminal content of the M-SHIME units, 42 h after inoculation with fecal samples of different human subjects: healthy, UC remission and UC relapse (n = 4)

	Healthy	UC remission	UC relapse
Acetate	54.0 \pm 3.8	40.7 \pm 4.9	46.1 \pm 6.0
Propionate	7.3 \pm 0.3	6.2 \pm 3.2	9.4 \pm 1.4
Butyrate	23.6 \pm 5.3	18.9 \pm 4.2	23.8 \pm 3.4
Valerate	0.6 \pm 0.6	1.6 \pm 0.8	0.7 \pm 0.6
Caproate	1.5 \pm 1.5	3.6 \pm 2.8	0.1 \pm 0.1
Branched SCFA	2.0 \pm 1.6	5.1 \pm 1.2	3.2 \pm 1.3
Total SCFA	89.1 \pm 2.5	76.2 \pm 4.6	83.3 \pm 7.6

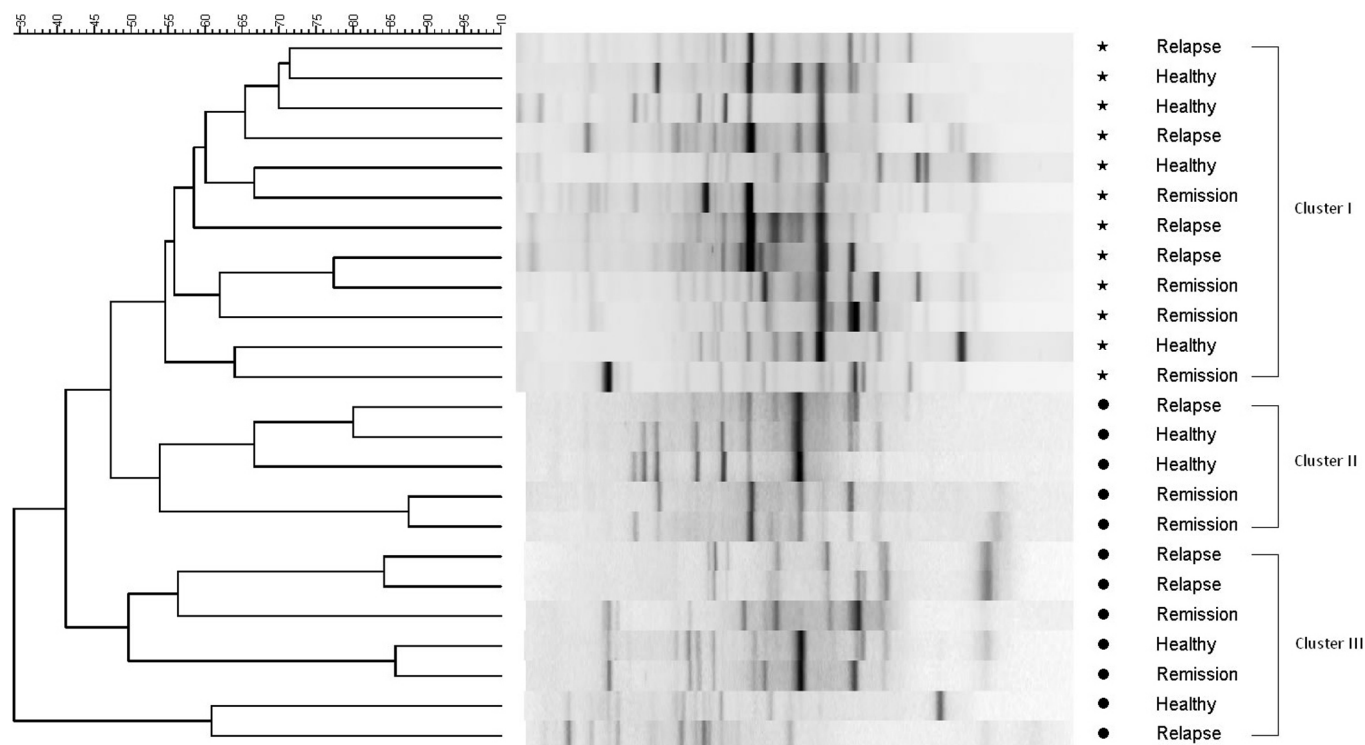


Figure 1 | Dice cluster analysis of universal DGGE gel profiles from *in vitro* luminal and mucosal communities of the M-SHIME colonized with samples derived from healthy subjects, or from UC patients in remission or relapse. The luminal samples are indicated by stars (*) and the mucosal samples are indicated by full circle (•). The dendrogram can be divided into three clusters: Cluster I: mucosal samples (54.61% similarity). Cluster II: luminal samples (53.89% similarity). Cluster III: luminal samples (41.15% similarity). Metric scale indicates degree of similarity in percentages.

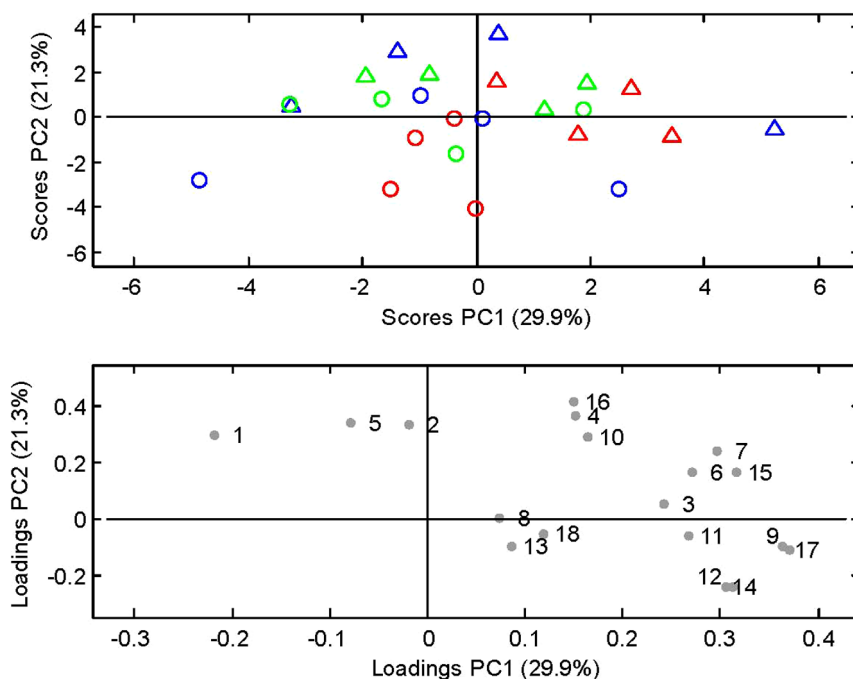


Figure 2 | Principal Component Analysis of the quantitative PCR measurements illustrated by PC1 and PC2 (29.9% and 21.3% of explained variance, respectively). Score plot showing the M-SHIME luminal (Δ) and mucosal (\circ) communities. Sources of the communities are indicated by green for healthy subjects, blue for UC patients in remission and red for UC patients in relapse. Loading plot indicating each of the measured bacterial taxa as determined by quantitative Real-Time PCR. 1. *B. bifidum*; 2. *B. adolescentis*; 3. *B. pseudocatenulatum*; 4. *Bifidobacterium* spp.; 5. *Lactobacillus* spp.; 6. *C. leptum* subgroup; 7. *C. coccoides* group; 8. *F. prausnitzii*; 9. *Desulfovibrio* spp.; 10. *Akk. muciniphila*; 11. *Firmicutes*; 12. *Bacteroidetes*; 13. *Roseburia* spp.; 14. *Bacteroides* spp.; 15. *Alistipes* spp.; 16. *Actinobacteria*; 17. *Bac. fragilis* group; 18. *Clostridiaceae/Eubacterium*.



Table 2 | Preference of bacterial taxa to colonize the mucosal compartment, expressed as ratio of the relative quantities in mucosal and luminal compartments of the M-SHIME

Bacterial taxa	Ratios mucus/lumen (%) ^a		
	Health subjects	UC remission	UC relapse
<i>Firmicutes</i>	100.36 (±1.23)	100.46 (±1.64)	99.85 (±0.89)
• <i>Clostridiaceae</i> ^b / <i>Eubacterium</i>	103.18 (±29.64)	117.47 (±19.49)	79.53 (±7.99)
• <i>Clostridium leptum</i> subgroup	96.33 (±8.43)	83.81 (±5.12)*	82.39 (±3.35)*
◦ <i>Faecalibacterium prausnitzii</i>	102.62 (±13.35)	83.75 (±4.22)*	93.91 (±4.97)
• <i>Clostridium coccooides</i> group	88.47 (±10.94)	74.10 (±11.74)	66.81 (±10.73)*
◦ <i>Roseburia</i> spp.	108.01 (±7.70)	137.83 (±12.28)*	146.06 (±41.24)
• <i>Lactobacillus</i> spp.	94.70 (±8.85)	81.32 (±2.77)**	68.59 (±7.64)*
<i>Bacteroidetes</i>	99.98 (±2.84)	106.52 (±9.69)	94.36 (±7.57)
• <i>Bacteroides</i> spp.	98.44 (±2.87)	112.93 (±9.33)	85.28 (±5.06)
◦ <i>Bac. fragilis</i> group	93.95 (±7.55)	107.24 (±14.33)	75.48 (±8.88)
• <i>Alistipes</i> spp.	65.05 (17.58)	68.12 (±11.76)	71.91 (±8.47)*
<i>Actinobacteria</i>	76.29 (13.79)	55.39 (2.88)***	52.01 (16.96)
• <i>Bifidobacterium</i> spp.	94.60 (±3.12)	91.24 (±1.53)**	84.63 (±4.28)**
◦ <i>B. bifidum</i>	93.99 (±3.47)	106.37 (±6.97)	84.48 (±3.35)*
◦ <i>B. adolescentis</i>	89.52 (±4.61)	83.68 (±1.37)***	67.61 (±16.58)
◦ <i>B. pseudocatenulatum</i>	101.27 (±4.68)	79.79 (±3.55)**	94.60 (±15.00)
<i>Proteobacteria</i>			
• <i>Desulfovibrio</i> spp.	101.19 (±1.75)	101.22 (±4.53)	92.74 (±3.89)
<i>Verrucomicrobia</i>			
• <i>Akkermansia muciniphila</i>	85.48 (±6.90)	73.15 (±12.19)	86.18 (±5.10)

^aRatios (%) calculated as 100**mucosal samples/luminal samples*, hence values below 100% indicates low adherence capacity to mucus, while values above 100% indicate high adherence capacity to mucus.

^bIncludes Clusters I, III, IV, XIVa, XIVb.

Asterisks (*) indicate significant differences between mucosal and luminal samples (**P*<0.05 and ***P*<0.01). All calculated data are means ± SEM.

intestinal microbial ecosystems of healthy subjects and UC patients, either in relapse or in remission. This model allows investigation of differences within the luminal content as well as at the artificial intestinal mucosal surface^{23,24}. The impact of the human host on the microbial composition is eliminated, thus allowing focus on intrinsic features of the gut microbial populations. However, as any model, the M-SHIME has its limitations, and it should be noted

that the bacterial communities colonizing an in vitro fermentor can never be made completely identical to those present in humans due to e.g. possible loss of species during freezing, and altered availability of nutrients leading to changes in the competitive advantages of other species.

Still, in line with recent *in vivo*^{25,26} and *in vitro* studies^{27,28}, we have demonstrated that also in the M-SHIME model, the in vitro mucosal

Table 3 | Relative abundance of bacteria derived from UC patients compared to healthy subjects

Bacterial taxa	Lumen		Mucus	
	UC remission	UC relapse	UC remission	UC relapse
<i>Firmicutes</i>	98.99 (±2.34)	101.92 (±0.52)	99.02 (±0.96)	101.43 (±0.40)
• <i>Clostridiaceae</i> ^c / <i>Eubacterium</i>	111.60 (±13.44)	142.63 (±8.74)*	131.70 (±9.89)	120.27 (±13.98)
• <i>Clostridium leptum</i> subgroup	105.94 (±9.04)	120.45 (±3.06)	95.21 (±10.49)	106.03 (±4.53)
◦ <i>Faecalibacterium prausnitzii</i>	120.28 (±7.78)	125.79 (±3.57)	103.39 (±2.32)	122.12 (±5.42)
• <i>Clostridium coccooides</i> group	97.68 (±14.02)	119.86 (±6.22)	69.89 (±23.95)	94.02 (±16.97)
◦ <i>Roseburia</i> spp.	103.12 (±7.65)	72.29 (±11.66)	133.15 (±19.83)	89.96 (±24.74)
• <i>Lactobacillus</i> spp.	109.74 (±3.52)	80.06 (±12.88)	96.27 (±4.42)	57.99 (±8.93)***
<i>Bacteroidetes</i>	95.33 (±11.68)	107.10 (±4.71)	98.92 (±6.41)	100.04 (±4.25)
• <i>Bacteroides</i> spp.	93.35 (±11.66)	110.06 (±6.83)	104.27 (±6.83)	94.82 (±6.63)
◦ <i>Bac. fragilis</i> group	94.12 (±15.12)	113.49 (±8.76)	103.68 (±14.08)	88.68 (±6.82)
• <i>Alistipes</i> spp.	100.97 (±11.46)	111.57 (±6.01)	100.60 (±19.04)	118.90 (±18.49)
<i>Actinobacteria</i>	101.99 (±7.42)	100.10 (±3.65)	74.06 (±8.91)	68.72 (±23.89)
• <i>Bifidobacterium</i> spp.	99.97 (±3.72)	97.65 (±2.65)	96.53 (±4.95)	89.04 (±4.22)*
◦ <i>B. bifidum</i>	71.84 (±24.63)	79.50 (±11.98)	75.73 (±24.27)	71.53 (±11.61)
◦ <i>B. adolescentis</i>	112.86 (±4.80)	89.80 (±15.22)	106.56 (±5.15)	76.15 (±23.01)
◦ <i>B. pseudocatenulatum</i>	113.94 (±7.96)	96.16 (±22.55)	99.55 (±8.11)	90.74 (±18.72)
<i>Proteobacteria</i>				
• <i>Desulfovibrio</i> spp.	117.09 (±17.88)	120.72 (±5.61)	117.92 (±18.33)	111.03 (±4.90)
<i>Verrucomicrobia</i>				
• <i>Akkermansia muciniphila</i>	90.88 (±19.54)	79.57 (±17.82)	85.11 (±24.57)	73.99 (±14.50)

All numbers are average ± SEM of the four samples in each UC group of either lumen or mucus. The relative abundance values (%) are normalized to healthy controls (set to 100).

^cIncludes Clusters I, III, IV, XIVa, XIVb.

Asterisks (*) designate a significant difference from the healthy control group (**P* < 0.05 and ****P* < 0.001).

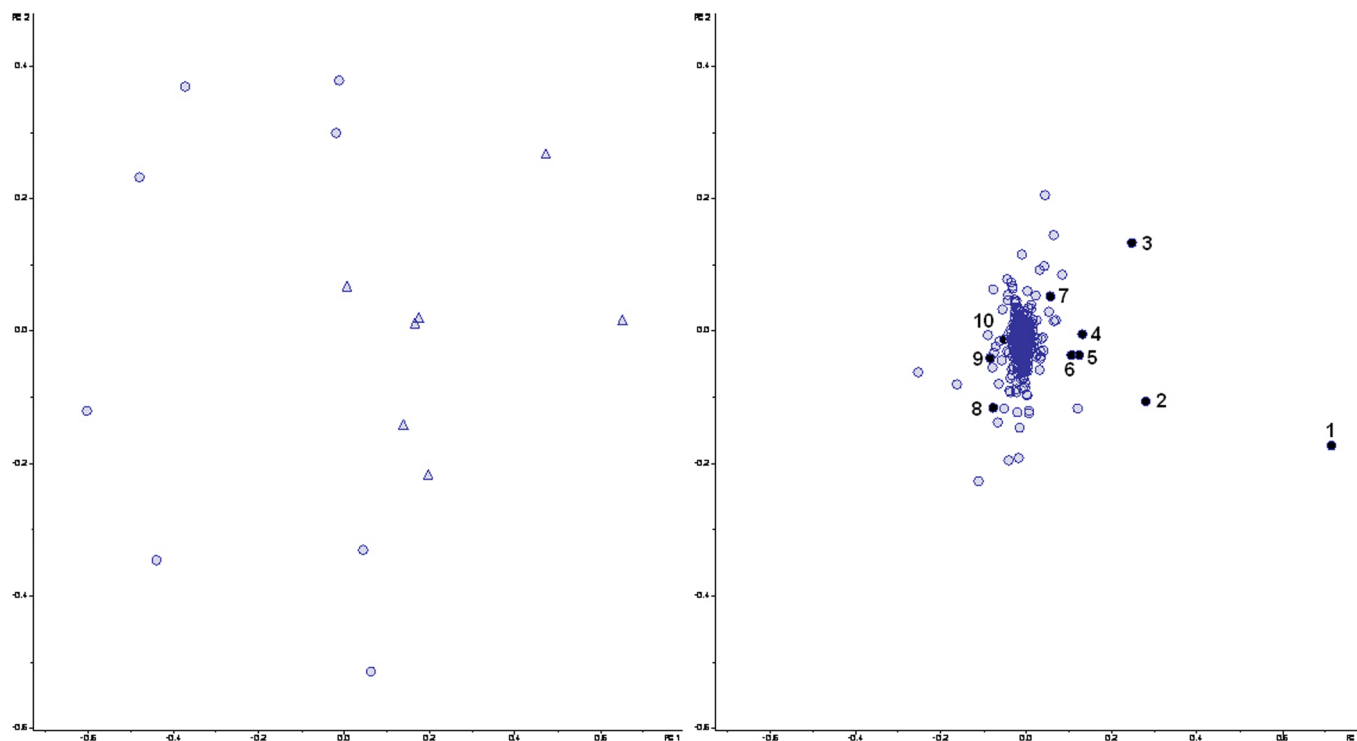


Figure 3 | Principal Component Analysis of LCMS data from the mucosal M-SHIME samples after colonization with microbiota derived from either healthy subjects (○) or UC patients in relapse (△). Score (left) and loading (right) plots are shown. PC1 and PC2 explain 29.1% and 18.6% of the variance, respectively. Numbers from 1 to 10 in the loading plot correspond to metabolite candidates enriched in the M-SHIME mucin-covered microcosms. Masses of the candidates are given in Table 4.

microbial community differs from the luminal one (Figure 1), with a tendency of specific butyrate-producing bacteria (e.g. *Roseburia* spp.) being abundant members of the mucosal microbiota (Table 2 and Figure 2). In samples from healthy people, the difference

between mucosal and luminal populations was more clearly seen by DGGE than by qPCR, probably reflecting that by qPCR only the subpopulations targeted by the selected primers are seen. The luminal and mucosal bacteria have previously been demonstrated to

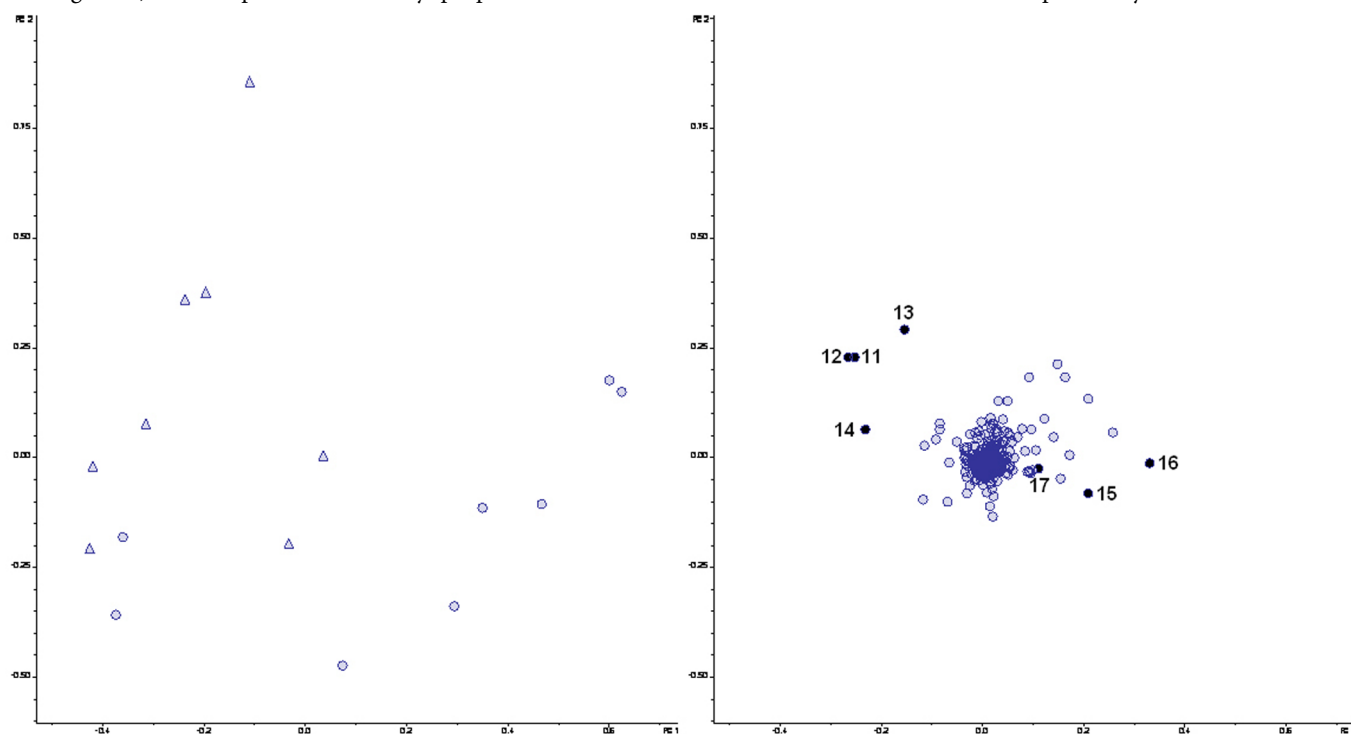


Figure 4 | Principal Component Analysis of the LCMS data from the luminal M-SHIME samples after colonization with microbiota derived from healthy subjects (○) or UC patients in relapse (△). Score (left) and loading (right) plots are shown. PC1 and PC2 explain 26.2% and 21.8% of the variance, respectively. Numbers from 11–17 in the loading plot correspond to metabolite candidates that are enriched in the luminal M-SHIME samples. Masses of the candidates are given in Table 5.



Table 4 | Annotated metabolites, which differ between healthy subjects and UC patients in relapse (mucus)

Enriched in UC relapse						
No.	Metabolite candidate	M _{PCA} (Da)/RT (min)	M _{LCMS} (Da)	M _{HMDB} (Da)	Error (mDa)	P values
1	Monounsaturated fatty acids (C18)	281.5/6	281.248569	281.248627	0.058	P<0.05
2	Polyunsaturated fatty acids (C18)	279.5/6	279.232812	279.232971	0.159	P<0.05
3	Secondary bile acids	391.5/4	391.285401	391.285400	0.001	P<0.05
4	Salicylic acid (drug)	194.5/2	194.046042	194.045883	0.159	P<0.001
5	Monounsaturated fatty acids (C18)	282.5/6	281.248569	281.248627	0.047	P<0.05
6	Aminosalicylic acid (drug metabolite) or 3-Hydroxyanthranilic acid (oxidation product of tryptophan metabolism)	152.5/1	152.035358	152.035309	0.049	P<0.01
7	Product of phenylalanine metabolism	149.5/3	149.060764	149.060806	0.042	P<0.01
Enriched in healthy subjects						
No.	Metabolite candidate	M _{PCA} (Da)	M _{LCMS} (Da)	M _{HMDB} (Da)	Error (mDa)	P values
8	Tryptophan	203.5/2	203.082491	203.082596	0.105	P<0.05
9	Phenylalanine	164.5/1	164.071619	164.071701	0.082	P<0.005
10	Hydroxyphenyllactic acid or 3-(3-hydroxyphenyl)-3-hydroxypropanoic acid	181.5/2	181.050629	181.050629	0.531	P<0.05

Numbers from 1–10 correspond to the metabolite marked in the loading plot Figure 3. M_{PCA} designates mass taken from PCA; RT designates retention time bucket of the PCA; M_{LCMS} designates mass taken from LCMS analysis of test samples; M_{HMDB} designates mass given by Human Metabolome Data Base; 'Error' designates the mass difference between measured M_{LCMS} and found M_{HMDB}.

display different roles in the host, and it has been proposed that the mucosal microbiota is more involved in interaction with the epithelial and immune cells than the luminal microbiota, because it resides closer to the intestinal epithelial cells^{29,30}. Hence, an altered mucosal microbial community may play an important role in dysregulated immune responses.

In spite of a limited sample size, we found a number of statistically significant differences between microbial communities derived from healthy people, UC patients in remission, and UC patients in relapse, respectively. For samples from UC patients a significantly lower proportion of lactobacilli and bifidobacteria residing in the mucus-microcosm than in the lumen was observed, while this was not the case for healthy microbiotas (Table 2). Notably, this was observed for UC patients in remission as well for those in relapse, indicating that the impaired ability of the lactic acid bacteria to adhere to mucus is present also when UC patients are free of severe symptoms. However, when directly comparing 'mucosal' populations from M-SHIME colonized with microbiota from UC patients to those colonized with healthy microbiotas, only patients in relapse had a significantly lower amount of bifidobacteria and lactobacilli than

found in the 'healthy' samples (Table 3). This could be due to the fact that microbiota from UC patients in relapse in general contained lower amounts of lactic acid bacteria than microbiota derived from either healthy people or UC patients in remission. Species or strain specific mucus adhesion promoting proteins have been reported in several bifidobacteria and lactobacilli^{6,31–35}. The expression of adhesion molecules may be changed in the lactic acid producing bacteria derived from UC patients, hence their inability to colonize the mucus *in vitro*. However, we would expect that host-induced differences in bacterial gene expression profiles would no longer prevail after 42 hours in the gut model. Alternatively, an altered composition of the species of lactobacilli and bifidobacteria derived from UC patients may explain the decreased ability of these groups to adhere to the mucin-microcosms of the M-SHIME. A third explanation may be that within a given species, the strains of lactic acid bacteria present in UC patients are less capable of adhesion to mucins than their counterparts present in healthy subjects, perhaps due to minor genetic differences in adhesion-relevant genes.

Bifidobacteria and lactobacilli are believed to play important roles in promoting intestinal health^{36–43}. The observed depletion of bifido-

Table 5 | Annotated metabolites, which differ between healthy subjects and UC patients in relapse (lumen)

Enriched in UC relapse						
No.	Metabolite candidate	M _{PCA} (Da)/RT (min)	M _{LCMS} (Da)	M _{HMDB} (Da)	Error (mDa)	P values
11	Secondary bile acids	391.5/4	391.285527	391.285400	0.127	P<0.01
12	Salicylic acid (drug)	194.5/2	194.046042	194.045993	0.110	P<0.001
13	Aminosalicylic acid (drug metabolite) or 3-Hydroxyanthranilic acid (oxidation product of tryptophan metabolism)	152.5/1	152.035358	152.035309	0.052	P<0.05
14	Product of phenylalanine metabolism	149.5/3	149.060764	149.060806	0.122	P<0.001
Enriched in healthy subjects						
No.	Metabolite candidate	M _{PCA} (Da)	M _{LCMS} (Da)	M _{HMDB} (Da)	Error (mDa)	P values
15	Tryptophan	203.5/2	203.082491	203.082596	0.278	P<0.001
16	Phenyllactic acid or 4-methoxyphenylacetic acid or desaminotyrosine	165.5/3	165.055687	165.055710	0.023	P<0.05
17	Phenylglycine	150.5/2	150.056153	150.056046	0.107	P<0.001

Numbers from 11–17 correspond to the metabolite marked in the loading plot Figure 4. M_{PCA} designates mass taken from PCA; RT designates retention time bucket of the PCA; M_{LCMS} designates mass taken from LCMS analysis of test samples; M_{HMDB} designates mass given by Human Metabolome Data Base; 'Error' designates the mass difference between measured M_{LCMS} and found M_{HMDB}.



bacteria and lactobacilli in UC patients in relapse, which is in line with a number of previous reports^{44–46}, is likely to have a consequence for colonic health. It is, however, not possible from the given data to conclude whether the impaired adhesion capacity of lactic acid bacteria derived from UC patients is part of the cause or part of the effect of the disease. It may be that the mucus layers in the intestines of the UC patients have selected for populations of lactic acid bacteria, which are less optimized to adhere to the ‘healthy’ mucin of the M-SHIME.

Also the ability of the butyrate-producing clostridial groups *C. coccoides* and *C. leptum* to colonize the mucin-covered microcosms of the M-SHIME was found to be lower in bacterial communities from UC patients than in those originating from healthy subjects, although for UC patients remission, this was only statistically significant for the *C. leptum* group (Table 2). This may be linked to the lower abundance of lactobacilli and bifidobacteria in the microcosms, since these species produce acetate and/or lactate, which is subsequently utilized by the given clostridial groups. In contrast to the *C. coccoides* group and the *C. leptum* subgroup, the butyrate-producing *Roseburia* spp. in microbiotas originating from UC patients demonstrated a high presence mucin-microcosms (Table 2), indicating that these species, which are known to be able to degrade complex carbohydrates⁴⁷, are not dependent on the presence of lactate and acetate as seen for their clostridial relatives. Hence, the low abundance of the clostridial groups within the mucin-microcosms may create a free ecological niche allowing for excessive colonization of *Roseburia* spp.

Metabolomic (LCMS) analysis revealed that the microbiotas from healthy subjects and from UC patients in remission displayed very similar metabolisms, while the metabolism of bacterial communities from UC patients in relapse was clearly different from these two groups (Figure 3, 4, S1, S2, S3 and S4). We found that metabolism of bile acids, tryptophan and phenylalanine were altered in luminal as well as mucosal samples derived from UC patients in relapse as compared to healthy subjects (Table 4 and 5). The presence of drugs and drug metabolites in samples from UC patients in relapse was expected, since all four patients received mesalazine (5-aminosalicylic acid).

In the human body, most bile acids are actively reabsorbed from the ileum and returned to the liver. However, a small fraction of bile acids escape enterohepatic circulation and enter the colon where bacteria metabolize the bile acids primarily by deconjugation and oxidation of hydroxyl groups. Bile salt hydrolysis is carried out by a broad spectrum of intestinal bacteria^{48,49}. However, the specificity of hydroxysteroid dehydrogenase (HSDH) varies depending on bacterial species and may either be specific for the 3-, 7-, and/or 12-hydroxy groups of bile acids leading to different secondary bile acids. Specific HSDHs have primarily been detected in a number of *Clostridium* and *Eubacterium* species belonging to either cluster I, IV (*C. leptum* subgroup), XIVa (*C. coccoides* group) or XIb^{49,50}. As we demonstrated significantly higher levels of *Clostridiaceae/Eubacterium* in the luminal samples from UC patients in relapse than in healthy subjects (Table 3), this could partly explain the observed enrichment of secondary bile acids. High levels of secondary bile acids such as deoxycholic acids (primarily produced by species belonging to *Clostridiaceae*) can be detrimental for colon health⁵¹.

Phenylalanine was more abundant in mucosal samples from the M-SHIME colonized with microbiota from healthy subjects, than in those colonized with samples from UC patients (Table 4). Products of phenylalanine that are normally metabolized by intestinal bacteria undergo a variety of processes in the body, where they may be detoxified by either glucuronide or sulphate conjugation in the gut mucosa and liver, or remain unabsorbed and voided in feces⁵². Production of phenolic compounds by proteolytic and peptidolytic activities of the intestinal bacteria has previously been associated with various dis-

eases including cancer and UC⁵². Previous studies have shown that species belonging to the genera *Clostridium* and *Bacteroides* have a high capacity to ferment phenylalanine to phenolic compounds such as phenylpropionate, phenylacetate and/or phenyllactate^{53,54}. Here, we observed higher levels of clostridia in samples derived from UC patients than in samples from healthy subjects (Table 3). Hence, we speculate that the enrichment of products of phenylalanine metabolism in mucosal and luminal samples derived from UC patients in relapse could be a result of the higher abundance of these bacterial groups (Table 4 and 5).

Also tryptophan levels were higher in samples from the M-SHIME colonized with microbiota from healthy subjects than when it was colonized with microbiota from UC patients in relapse (Table 4 and 5). In line with this, previous studies have revealed that after fermentation using inocula from healthy subjects, no products of tryptophan metabolism could be detected in the system^{52,54}.

Finally, we observed that unsaturated fatty acids (FA) were significantly higher in mucus compartments colonized with bacteria from UC patients in relapse than in those colonized with ‘healthy’ bacterial communities (Table 4). Previous metabolomic research has revealed changes of FA in serum of UC patients⁵⁵, and has suggested that these changes could be caused by increased endogenous biosynthesis of polyunsaturated fatty acids (PUFA) and by increased lipolysis initiated by cytokines during the inflammatory response. Based on the present work, we speculate that the altered levels of FA in serum UC patients in relapse compared to healthy subjects could be originating from the intestinal microbial metabolism.

In conclusion, our data suggest that the significantly altered intestinal bacterial community present in UC patients in relapse results in a significantly altered bacterial metabolic profile. The observed bacterial alterations are suggested to result in increased metabolism of phenylalanine and tryptophan in microbial communities from UC patients in relapse. While UC patients in remission display microbiotas and metabolomes very similar to those of healthy subjects, the lactic acid bacteria present in patients in remission are, similar to those from the relapse samples, significantly impaired in their ability to adhere to the mucus microcosms of the M-SHIME. This may be due to a different composition or a different genetic makeup of the lactic acid bacteria present in all UC patients, which may play a role in the etiology of this disease. We suggest that probiotic therapy for UC patients should not exclusively aim at increasing the amount of lactic acid bacteria present in the gut, which has previously proved helpful⁵⁶, but also at replacing the existing lactic acid bacteria with other strains/isolates with better capacity for mucosal adhesion.

Methods

Human volunteers and clinical characteristics of UC patients. Fecal samples were obtained from 8 patients with UC and 4 healthy controls⁵⁷. Within the UC group, 4 patients were in clinical remission and 4 patients had active disease at the time of sampling according to clinical and endoscopic criteria⁵⁸. The study was performed in accordance with the Second Helsinki Declaration, reported to the Danish Data Protection Agency and approved by the Regional Ethics Committee. Written informed consent was obtained from each participant under a protocol approved by the Danish National Committee on Biomedical Research Ethics. All four patients with active UC were treated with mesalazine (5-aminosalicylic acid). Two patients with inactive UC received mesalazine, one patient received olsalazine (6-hydroxybenzoate)-salicylic acid, and one received no anti-inflammatory treatment. None of the participants had been treated with antibiotics for at least 2 months before enrolment and there was no significant difference ($P = 0.32$) in the mean age of the participants when comparing the 3 groups.

Sample collection and processing. Stool samples were collected in airtight containers and stored at 4°C (limited storage time was encouraged⁵⁹) until delivery to the laboratory. Feces were homogenized in glycerol to give a 25% feces/glycerol slurry. This was performed in an anaerobic cabinet (Macs Work Station, Don Whitley, containing 10% H₂, 10% CO₂, and 80% N₂). The processed samples were stored at –80°C until further analysis.

Growth medium and chemicals. Unless stated otherwise, chemicals were obtained from Sigma (Bornem, Belgium). The M-SHIME feed contained 1.0 g/l arabinogalactan, 2.0 g/l pectin, 1.0 g/l xylan, 3.0 g/l starch, 0.4 g/l glucose, 3.0 g/l



yeast extract, 1.0 g/l peptone, 4.0 g/l mucin, and 0.5 g/l cysteine. Pancreatic juice contained 12.5 g/l NaHCO₃, 6.0 g/l bile salts (Difco, Bierbeek, Belgium) and 0.9 g/l pancreatin. Mucin agar was prepared by boiling autoclaved distilled H₂O containing 5% porcine mucin type II and 1% agar. The pH was adjusted to 6.8 with 10 M NaOH.

M-SHIME. Analysis in the M-SHIME dynamic gut model was carried out as previously described²⁷ at two different occasions with six participants for each 42-hours run (two healthy, two UC patients in remission and two UC patients in relapse). The position (vessel) of the inocula from either healthy subjects or UC patients was changed for each run.

Microbial activity in terms of short-chain fatty acids (SCFA). Acetate, propionate, butyrate, valerate, caproate and branched SCFA (isobutyrate, isovalerate and isocaproate) were measured as described previously⁶⁰.

Extraction of bacterial DNA. Before extraction of the mucosal samples, the samples were heated for 15 min at 55°C to make the agar soluble. Subsequently, DNA was extracted from thawed samples using the QIAamp DNA Stool mini kit (Qiagen, Hilden, Germany) with a bead beater step in advance, as previously described⁶¹. For each sample, DNA was extracted in duplicates. The purified DNA was stored at -20°C until use.

PCR amplification for DGGE. Aliquots (10 µL) of purified DNA (5 ng/µL of pooled DNA from the duplicate DNA extractions) were applied to the following to give a 50 µL PCR reaction mixture: 20 µL of 5 PRIME MasterMix (2.5×) (VWR & Bie & Berntsen) and 10 pmol of each of the primers (Eurofins MWG Synthesis GmbH, Ebersberg, Germany). Primers HDA1-GC/HDA2⁶² targeting 16S rRNA genes from all bacteria were used in a touchdown PCR as previously described⁶³.

Analysis of luminal and mucosal microbiota by DGGE. DGGE was carried out as described previously⁶⁴ using a Dcode™ Universal Mutation Detection System instrument and gradient former model 475 according to the manufacturer's instructions (Bio-Rad Labs, Hercules, California). The 9% polyamide gels were made with denaturing gradients ranging from 25% to 65%. The 100% denaturing solution contained 40% formamide and 7 M urea. Thirteen microlitres PCR products were mixed with 3 µL loading dye before loading. Gels were run in 1 x TAE at 60 °C for 16 h at 36 V, 28 mA, stained with ethidium bromide for 15 min, destained for 20 min, and viewed by UV-B trans illumination at 302 nm (Bio-Rad). The BioNumerics software, version 4.60 (Applied Maths, Sint-Martens-Latem, Belgium) was used for identification of bands and normalization of band patterns from DGGE gels. DGGE gels were normalized by an assigned marker (developed in our laboratory). A cluster analysis was performed based on Dice coefficient of similarity (weighted) using the unweighted pair group method and the arithmetic averages clustering algorithm.

Quantitative PCR assay conditions. qPCR was performed on an ABI Prism 7900 HT from Applied Biosystems. The amplification reactions were carried out in a total volume of 11 µL containing: 5.50 µL (SYBR[®] Green, Applied Biosystems), primers (each at 200 nM concentration) (Eurofins MWG Synthesis GmbH), 2 µL template DNA, and Nuclease-free water (Qiagen) purified for PCR. The amplification was carried out as previously described⁶⁵. DNA (5 ng/µL) from the duplicate DNA extractions of each sample was used for the qPCR.

Quantitative PCR primer and data handling. The primers specific to regions of the 16S rRNA genes of 20 selected bacterial taxa are listed in Table S1 (supplementary data). The taxa were selected based on an expected relevance to human health, and the specificity of the primers under the given conditions has recently been verified⁶⁶. The relative quantities of gene targets encoding gene sequences of the bacterial taxa were calculated using 2^{-DeltaCt}, assuming primer efficiency at 1.0. Delta Ct is the Ct-values of the bacterial target normalized against Ct-values of the total bacterial population in a sample. Ct is the threshold cycle calculated by the ABI software (SDS version 2.2; Applied Biosystems, Foster City, California, USA) as the PCR cycle, where amplification signal exceeds the selected threshold value, also set by the ABI software. Prior to the quantification, standard curves were created using serial 10-fold dilutions of bacterial DNA extracted from one of the M-SHIME samples for all primer sets. Analysis of the standard curves allowed verification of PCR efficiency for the chosen PCR conditions. All primers were tested to confirm sensitivity and specificity using DNA from pure bacterial species (Table S2, supplementary data). The detection limit was set to 0.001% of the quantity of the total bacteria. Bacterial targets that could not be detected or were below the detection limit were set to one half of the detection limit for further calculations.

Metabolite detection & identification. Luminal samples from the M-SHIME were thawed on ice and subsequently centrifuged at 3000 g for 15 min at 4°C. Cold methanol (around -80°C) in a ratio 1 : 1 was added to the supernatant. Metabolites from the mucosal samples, due to the semi-solid form, were extracted with 2 ml of cold 50% methanol and centrifuged at 3000 g for 15 min at 4°C. This procedure was repeated twice. All of the samples were stored at -80°C until further analysis and centrifuged at 15000 g for 5 min at 4°C just before LCMS analysis. The analysis of metabolites was conducted as follows: a Dionex Ultimate 3000 RS liquid chromatograph (Dionex, Germering, Germany) coupled to a Bruker maXis time of flight mass spectrometer equipped with an electrospray interphase (Bruker Daltonics,

Bremen, Germany). Analytes were separated on Kinetex pentafluorophenyl column 50 x 2.10 mm, 2.6 µm, 100 Å (Phenomenex, USA), using the solvent system: A, 10 mM ammonium formate pH 3.5, and B, acetonitrile. Solvent programming was isocratic 0% B to 0 min followed by a linear gradient to 100% B at 7 min and 100% B at 8 min. Flow rate was 0.25 ml/min at 0 min, increased to 0.4 ml/min at 7 min. Solvent composition and flow were returned to initial conditions at 8.2 min. The oven temperature was 40°C. Injection volumes were 1 µL. The following electrospray interphase settings were used: nebulizer pressure 2 bar, drying gas 10 l/min, 200°C, capillary voltage 4000 V. Scan range was from 50 to 800 m/z. The main focus of this study was acids, thus samples were analyzed in negative mode.

To identify metabolites seen to separate given groups, the Human Metabolome Database (HMDB; Wishart et al. 2009) was used. Molecular formulas of the metabolites from the LCMS analysis were generated based on exact mass and isotopic pattern with Bruker Daltonics Software. Identification of metabolites was based on a very low measurement error (Tab.1, Tab.2; external & internal calibration and lock mass was used), compared to the data given in HMDB and further references to the microbial metabolism in the GI. In addition hydrophobic properties of the molecule, indicated by the retention time in the chromatograph, were taken into consideration.

Statistical analysis. Statistical analysis of the qPCR data was performed using OriginPro software (version 8.1; OriginLab Corporation, Northampton, USA). Normality and homogeneity of variances of the qPCR data were assessed using the Kolmogorov-Smirnov and the Levene's test, respectively. Log-transformations were performed for data that did not meet these criteria. T-testing was applied to identify significant differences in colonization ability using the ratio (proportion) of the given bacterial taxon present in the two communities (lumen and mucus) for the three groups (healthy, UC patients in remission and UC patients in relapse). Univariate ANOVA was used to determine significant differences between specific bacterial taxa comparing the three groups either from lumen or mucus. Where ANOVA indicated a significant difference, Fisher's least significant different test was used. The nonparametric Kruskal-Wallis test was used for datasets, which did not have homogeneity of variance or were not normally distributed even after log-transformation. Univariate ANOVA was applied to confirm that there was no age differences between the three disease groups. Tests were considered statistically significant if P-values lower than 0.05 were obtained. Principal Component Analysis (PCA) of qPCR data was carried out using LatentX[®] data analytical software (version 2.00, The Mathworks Inc., Copenhagen, Denmark). Differences in metabolite profiles were evaluated by PCA using Profile Analysis 2.0 by Bruker Daltonics. Data was grouped into buckets of 1 min and 1 m/z differences in the range from 0.5 to 9 min and 50 to 800 m/z and normalized by the sum of buckets in the analysis. P-values were calculated by univariate ANOVA ($\alpha = 0.05$) using the normalized values from the PCA. As for the qPCR analysis, tests were considered significant when P-values lower than 0.05 were obtained.

- Eckburg, P. B. *et al.* Diversity of the human intestinal microbial flora. *Science* **308**, 1635–1638 (2005).
- Zoetendal, E. G. *et al.* Mucosa-associated bacteria in the human gastrointestinal tract are uniformly distributed along the colon and differ from the community recovered from feces. *Appl. Environ. Microbiol.* **68**, 3401–3407 (2002).
- Johansson, M. E. V. *et al.* The inner of the two Muc2 mucin-dependent mucus layers in colon is devoid of bacteria. *Proc. Natl. Acad. Sci. U. S. A.* **105**, 15064–15069 (2008).
- Killer, J. & Marounek, M. Fermentation of mucin by bifidobacteria from rectal samples of humans and rectal and intestinal samples of animals. *Folia Microbiol. (Praha)*. **56**, 85–89 (2011).
- Kline, K. A., Falker, S., Dahlberg, S., Normark, S. & Henriques-Normark, B. Bacterial Adhesins in Host-Microbe Interactions. *Cell Host & Microbe* **5**, 580–592 (2009).
- Pretzer, G. *et al.* Biodiversity-based identification and functional characterization of the mannose-specific adhesin of *Lactobacillus plantarum*. *J. Bacteriol.* **187**, 6128–6136 (2005).
- Kornbluth, A. & Sachar, D. B. Ulcerative Colitis Practice Guidelines in Adults: American College of Gastroenterology, Practice Parameters Committee. *Am. J. Gastroenterol.* **105**, 501–523 (2010).
- Loftus, E. V. Clinical epidemiology of inflammatory bowel disease: Incidence, prevalence, and environmental influences. *Gastroenterol* **126**, 1504–1517 (2004).
- Sartor, R. B. Mechanisms of disease: pathogenesis of Crohn's disease and ulcerative colitis. *Nat. Clin. Pract. Gastroenterol. Hepatol* **3**, 390–407 (2006).
- Brown, S. J. & Mayer, L. The immune response in inflammatory bowel disease. *Am. J. Gastroenterol.* **102**, 2058–2069 (2007).
- Hanauer, S. B. Inflammatory bowel disease: epidemiology, pathogenesis, and therapeutic opportunities. *Inflamm. Bowel. Dis.* **12** Suppl 1, S3–S9 (2006).
- Larsson, J. M. *et al.* Altered O-glycosylation profile of MUC2 mucin occurs in active ulcerative colitis and is associated with increased inflammation. *Inflamm. Bowel Dis.* **17**, 2299–30 (2011).
- Pullan, R. D. *et al.* Thickness of Adherent Mucus Gel on Colonic Mucosa in Humans and Its Relevance to Colitis. *Gut* **35**, 353–359 (1994).
- Frank, D. N. *et al.* Molecular-phylogenetic characterization of microbial community imbalances in human inflammatory bowel diseases. *Proc. Natl. Acad. Sci. U. S. A.* **104**, 13780–13785 (2007).



15. Michail, S. *et al.* Alterations in the gut microbiome of children with severe ulcerative colitis. *Inflamm. Bowel Dis.* **18**, 1799–1808 (2012).
16. Qin, J. J. *et al.* A human gut microbial gene catalogue established by metagenomic sequencing. *Nature* **464**, 59–U70 (2010).
17. Sokol, H. *et al.* Low Counts of *Faecalibacterium prausnitzii* in Colitis Microbiota. *Inflamm. Bowel Dis.* **15**, 1183–1189 (2009).
18. Takaiishi, H. *et al.* Imbalance in intestinal microflora constitution could be involved in the pathogenesis of inflammatory bowel disease. *Int. J. Med. Microbiol.* **298**, 463–472 (2008).
19. Ouwehand, A. C., Suomalainen, T., Tolkkio, S. & Salminen, S. In vitro adhesion of propionic acid bacteria to human intestinal mucus. *Lait* **82**, 123–130 (2002).
20. Van den Abbeele, P. *et al.* In vitro model to study the modulation of the mucin-adhered bacterial community. *Applied Microbiology and Biotechnology* **83**, 349–359 (2009).
21. Ouwehand, A. C. *et al.* Resected human colonic tissue: New model for characterizing adhesion of lactic acid bacteria. *Clinical and Diagnostic Laboratory Immunology* **9**, 184–186 (2002).
22. Laparra, J. & Sanz, Y. Comparison of in vitro models to study bacterial adhesion to the intestinal epithelium. *Letters in Applied Microbiology* **49**, 695–701 (2009).
23. Van den Abbeele, P. *et al.* Incorporating a mucosal environment in a dynamic gut model results in a more representative colonization by lactobacilli. *Microbial Biotechnology* **5**, 106–115 (2011).
24. Van den Abbeele, P. *et al.* Microbial Community Development in a Dynamic Gut Model Is Reproducible, Colon Region Specific, and Selective for Bacteroidetes and Clostridium Cluster IX. *Applied and Environmental Microbiology* **76**, 5237–5246 (2010).
25. Hong, P. Y., Croix, J. A., Greenberg, E., Gaskins, H. R. & Mackie, R. I. Pyrosequencing-Based Analysis of the Mucosal Microbiota in Healthy Individuals Reveals Ubiquitous Bacterial Groups and Micro-Heterogeneity. *Plos One* **6**, e25042 (2011).
26. Nava, G. M., Friedrichsen, H. J. & Stappenbeck, T. S. Spatial organization of intestinal microbiota in the mouse ascending colon. *ISME Journal* **5**, 627–638 (2011).
27. Vermeiren, J. *et al.* Decreased colonization of fecal Clostridium coccoides/Eubacterium rectale species from ulcerative colitis patients in an in vitro dynamic gut model with mucin environment. *FEMS Microbiol. Ecol* **79**, 685–696 (2012).
28. Van den Abbeele, P. *et al.* Butyrate-producing Clostridium cluster XIVa species specifically colonize mucus in an in vitro gut model. *ISME J*, in press(2012).
29. Derrien, M. *et al.* Modulation of Mucosal Immune Response, Tolerance, and Proliferation in Mice Colonized by the Mucin-Degrader Akkermansia muciniphila. *Front Microbiol.* **2**, 1–14 (2011).
30. Van den Abbeele, P., Van de Wiele, T., Verstraete, W. & Possemiers, S. The host selects mucosal and luminal associations of coevolved gut microorganisms: a novel concept. *FEMS Microbiol. Rev.* **35**, 681–704 (2011).
31. Gilad, O., Svensson, B., Viborg, A. H., Stuer-Lauridsen, B. & Jacobsen, S. The extracellular proteome of Bifidobacterium animalis subsp lactis BB-12 reveals proteins with putative roles in probiotic effects. *Proteomics* **11**, 2503–2514 (2011).
32. Kankainen, M. *et al.* Comparative genomic analysis of Lactobacillus rhamnosus GG reveals pili containing a human-mucus binding protein. *Proc. Natl. Acad. Sci. U. S. A.* **106**, 17193–17198 (2009).
33. Pridmore, R. D. *et al.* The genome sequence of the probiotic intestinal bacterium Lactobacillus johnsonii NCC 533. *Proc. Natl. Acad. Sci. U. S. A.* **101**, 2512–2517 (2004).
34. Kleerebezem, M. *et al.* The extracellular biology of the lactobacilli. *FEMS Microbiol. Rev.* **34**, 199–230 (2010).
35. Van Tassel, M. L. & Miller, M. J. Lactobacillus Adhesion to Mucus. *Nutrients* **3**, 613–636 (2011).
36. Fooks, L. J. & Gibson, G. R. In vitro investigations of the effect of probiotics and prebiotics on selected human intestinal pathogens. *FEMS Microbiol. Ecol* **39**, 67–75 (2002).
37. Lee, J. H., Li, X. L. & O'Sullivan, D. J. Transcription Analysis of a Lantibiotic Gene Cluster from Bifidobacterium longum DJO10A. *Applied and Environmental Microbiology* **77**, 5879–5887 (2011).
38. Saulnier, D. M. *et al.* Exploring Metabolic Pathway Reconstruction and Genome-Wide Expression Profiling in Lactobacillus reuteri to Define Functional Probiotic Features. *Plos One* **6**, 1–14 (2011).
39. Chenoll, E. *et al.* Novel Probiotic Bifidobacterium bifidum CECT 7366 Strain Active against the Pathogenic Bacterium Helicobacter pylori. *Applied and Environmental Microbiology* **77**, 1335–1343 (2011).
40. Collado, M. C., Meriluoto, J. & Salminen, S. In vitro analysis of probiotic strain combinations to inhibit pathogen adhesion to human intestinal mucus. *Food. Res. Int.* **40**, 629–636 (2007).
41. Lee, Y. K., Puong, K. Y., Ouwehand, A. C. & Salminen, S. Displacement of bacterial pathogens from mucus and Caco-2 cell surface by lactobacilli. *Journal of Medical Microbiology* **52**, 925–930 (2003).
42. Hoarau, C., Lagaraine, C., Martin, L., Velge-Roussel, F. & Lebranchu, Y. Supernatant of Bifidobacterium breve induces dendritic cell maturation, activation, and survival through a Toll-like receptor 2 pathway. *Journal of Allergy and Clinical Immunology* **117**, 696–702 (2006).
43. Zeuthen, L. H. *et al.* Lactobacillus acidophilus induces a slow but more sustained chemokine and cytokine response in naive foetal enterocytes compared to commensal Escherichia coli. *BMC Immunol* **11**, 1–10 (2010).
44. Mylonaki, M., Rayment, N. B., Rampton, D. S., Hudspith, B. N. & Brostoff, J. Molecular characterization of rectal mucosa-associated bacterial flora in inflammatory bowel disease. *Inflamm. Bowel Dis.* **11**, 481–487 (2005).
45. Vignsnaes, L. K., Brynskov, J., Steenholdt, C., Wilcks, A. & Licht, T. R. Gram-negative bacteria account for main differences between faecal microbiota from patients with ulcerative colitis and healthy controls. *Benef. Microbes.* **3**, 287–97 (2012).
46. Macfarlane, S., Furrrie, E., Cummings, J. H. & Macfarlane, G. T. Chemotaxonomic analysis of bacterial populations colonizing the rectal mucosa in patients with ulcerative colitis. *Clin. Infect. Dis.* **38**, 1690–1699 (2004).
47. Flint, H. J., Duncan, S. H., Scott, K. P. & Louis, P. Interactions and competition within the microbial community of the human colon: links between diet and health. *Environmental Microbiology* **9**, 1101–1111 (2007).
48. Jones, B. V., Begley, M., Hill, C., Gahan, C. G. M. & Marchesi, J. R. Functional and comparative metagenomic analysis of bile salt hydrolase activity in the human gut microbiome. *Proc. Natl. Acad. Sci. U. S. A.* **105**, 13580–13585 (2008).
49. Ridlon, J. M., Kang, D. J. & Hylemon, P. B. Bile salt biotransformations by human intestinal bacteria. *J. Lipid Res.* **47**, 241–259 (2006).
50. Doerner, K. C., Takamine, F., Lavoie, C. P., Mallonee, D. H. & Hylemon, P. B. Assessment of fecal bacteria with bile acid 7 alpha-dehydroxylating activity for the presence of bai-like genes. *Appl. Environ. Microbiol.* **63**, 1185–1188 (1997).
51. McGarr, S. E., Ridlon, J. M. & Hylemon, P. B. Diet, anaerobic bacterial metabolism, and colon cancer - A review of the literature. *J. Clin. Gastroenterol.* **39**, 98–109 (2005).
52. Smith, E. A. & Macfarlane, G. T. Formation of phenolic and indolic compounds by anaerobic bacteria in the human large intestine. *Microb. Ecol.* **33**, 180–188 (1997).
53. Elsdon, S. R., Hilton, M. G. & Waller, J. M. End Products of Metabolism of Aromatic Amino-Acids by Clostridia. *Arch. Microbiol.* **107**, 283–288 (1976).
54. Smith, E. A. & Macfarlane, G. T. Enumeration of human colonic bacteria producing phenolic and indolic compounds: Effects of pH, carbohydrate availability and retention time on dissimilatory aromatic amino acid metabolism. *J. Appl. Bacteriol.* **81**, 288–302 (1996).
55. Hengstermann, S. *et al.* Altered status of antioxidant vitamins and fatty acids in patients with inactive inflammatory bowel disease. *Clin. Nutr.* **27**, 571–578 (2008).
56. Zocco, M. A. *et al.* Efficacy of Lactobacillus GG in maintaining remission of ulcerative colitis. *Aliment. Pharmacol. Ther.* **23**, 1567–1574 (2006).
57. Langholz, E., Munkholm, P., Davidsen, M. & Binder, V. Course of Ulcerative Colitis - Analysis of Changes in Disease-Activity Over Years. *Gastroenterol* **107**, 3–11 (1994).
58. Binder, V. A Comparison Between Clinical State, Macroscopic and Microscopic Appearances of Rectal Mucosa, and Cytologic Picture of Mucosal Exudate in Ulcerative Colitis. *Scand. J. Gastroenterol.* **5**, 627–632 (1970).
59. Ott, S. J. *et al.* In vitro alterations of intestinal bacterial microbiota in fecal samples during storage. *Diagn. Microbiol. Infect. Dis.* **50**, 237–245 (2004).
60. De Weirtd, R. *et al.* Human faecal microbiota display variable patterns of glycerol metabolism. *FEMS Microbiol. Ecol* **74**, 601–611 (2010).
61. Leser, T. D., Lindecrona, R. H., Jensen, T. K., Jensen, B. B. & Moller, K. Changes in bacterial community structure in the colon of pigs fed different experimental diets and after infection with Brachyspira hyodysenteriae. *Appl. Environ. Microbiol.* **66**, 3290–3296 (2000).
62. Walter, J. *et al.* Detection and identification of gastrointestinal Lactobacillus species by using denaturing gradient gel electrophoresis and species-specific PCR primers. *Appl. Environ. Microbiol.* **66**, 297–303 (2000).
63. Petersen, A. *et al.* Analysis of the intestinal microbiota of oligosaccharide fed mice exhibiting reduced resistance to Salmonella infection. *Beneficial Microbes* **3**, 271–281 (2010).
64. Bernbom, N. *et al.* Comparison of methods and animal models commonly used for investigation of fecal microbiota: Effects of time, host and gender. *J. Microbiol. Methods* **66**, 87–95 (2006).
65. Vignsnaes, L. K., Holck, J., Meyer, A. S. & Licht, T. R. In vitro fermentation of sugar beet arabinose-oligosaccharides by fecal microbiota obtained from patients with ulcerative colitis to selectively stimulate the growth of Bifidobacterium spp. and Lactobacillus spp. *Appl. Environ. Microbiol.* **77**, 8336–8344 (2011).
66. Bergstrom, A. *et al.* Introducing Gut Low-Density Array (GULDA) - a validated approach for qPCR-based intestinal microbial community analysis. *FEMS Microbiol. Lett.* **337**, 38–47 (2012).

Acknowledgements

We thank Kate Vibefeldt at the Technical University of Denmark, and Birgit Kristensen Herlev Hospital, Denmark, for excellent technical assistance. Pieter Van den Abbeele is a Postdoctoral fellow from FWO-Vlaanderen (Research Foundation of Flanders, Belgium). This work was financed by the Danish Council for Strategic Research (grant no. 2101-06-0067), Project 'Healthy Growth' at Oeresund Food Network, Technical University of Denmark and a GOA project (BOF12/GOA/008) from Ghent University.

Author contributions

L.K.V., P.v.d.A. and T.R.L. conceived of the experiment and participated in its design. L.K.V. carried out the qPCR and DGGE, P.v.d.A. carried out the SCFA analysis, while K.S. and



H.L.F. carried out the metabolome analysis. P.v.d.A., T.v.d.W., J.V. and L.K.V. were responsible for the M-SHIME model, while C.S. and J.B. were responsible for collection of fecal microbiotas from U.C. patients. L.K.V., P.v.d.A., K.S. and T.R.L. drafted the manuscript together. All authors read, commented, and approved of the manuscript.

Additional information

Supplementary information accompanies this paper at <http://www.nature.com/scientificreports>

Competing financial interests: The authors declare no competing financial interests.

License: This work is licensed under a Creative Commons Attribution-NonCommercial-NoDerivs 3.0 Unported License. To view a copy of this license, visit <http://creativecommons.org/licenses/by-nc-nd/3.0/>

How to cite this article: Vigsnaes, L.K. *et al.* Microbiotas from UC patients display altered metabolism and reduced ability of LAB to colonize mucus. *Sci. Rep.* **3**, 1110; DOI:10.1038/srep01110 (2013).